THE JOURNAL OF BIOLOGICAL CHEMISTRY VOL. 289, NO. 18, pp. 12520–12534, May 2, 2014

Transcription of Angiogenin and Ribonuclease 4 Is Regulated by RNA Polymerase III Elements and a CCCTC Binding Factor (CTCF)-dependent Intragenic Chromatin Loop*

Received for publication, January 21, 2014, and in revised form, March 14, 2014 Published, JBC Papers in Press, March 21, 2014, DOI 10.1074/jbc.M114.551762

Jinghao Sheng[‡§], **Chi Luo**[‡], **Yuxiang Jiang**[‡], **Philip W. Hinds**[‡], **Zhengping Xu**[§1], **and Guo-fu Hu**[‡2]

From the [‡]*Molecular Oncology Research Institute, Tufts Medical Center, Boston, Massachusetts 02111 and* [§]*Institute of Environmental Medicine, Zhejiang University School of Medicine, Hangzhou 310058, China*

Background: Angiogenin and ribonuclease 4 share genetic regions with promoter activities, and both have growth and survival activity.
Results: RNA polymerase III elements and CTCF-dependent intragenic chromatin loop regulate the transcription.
Conclusion: Multiple layers of transcription regulation of this gene locus encode two functionally similar but distinctive proteins.
Significance: Elucidating how angiogenin and ribonuclease 4 are differentially transcribed help understand their biological activities.

Angiogenin (ANG) and ribonuclease 4 (RNASE4), two members of the secreted and vertebrate-specific ribonuclease superfamily, play important roles in cancers and neurodegenerative diseases. The *ANG* and *RNASE4* genes share genetic regions with promoter activities, but the structure and regulation of these putative promotes are unknown. We have characterized the promoter regions, defined the transcription start site, and identified a mechanism of transcription regulation that involves both RNA polymerase III (Pol III) elements and CCCTC binding factor (CTCF) sites. We found that two Pol III elements within the promoter region influence *ANG* and *RNASE4* expression in a position- and orientation-dependent manner. We also provide evidence for the presence of an intragenic chromatin loop between the two CTCF binding sites located in two introns flanking the *ANG* coding exon. We found that formation of this intragenic loop preferentially enhances *ANG* transcription. These results suggest a multilayer transcriptional regulation of *ANG* and *RNASE4* gene locus. These data also add more direct evidence to the notion that Pol III elements are able to directly influence Pol II gene transcription. Furthermore, our data indicate that a CTCF-dependent chromatin loop is able to differentially regulate transcription of genes that share the same promoters.

ANG,[3] the fifth member of the secreted and vertebrate-specific ribonuclease superfamily (1), is known to regulate angiogenesis and neurogenesis during development (2). It also plays important roles in a number of pathological conditions including cancers and neurodegenerative diseases by modulating cell growth and survival properties (3). ANG expression is up-regulated in various types of human cancers (4) where it has been shown to promote cancer progression (5) by stimulating both tumor angiogenesis (6) and cancer cell growth (7). Thus, ANG inhibitors are perceived to have the benefit of combining anti-angiogenesis therapy and chemotherapy as they will inhibit both cancer cell proliferation and angiogenesis (8).

In contrast to being up-regulated in cancers, *ANG* is down-regulated in amyotrophic lateral sclerosis (9), Parkinson disease (10), and Alzheimer disease (11). More importantly, loss-of-function mutations have been found in patients with amyotrophic lateral sclerosis and Parkinson disease (12–14), suggesting that ANG plays a role in neuron survival, and its deficiency is a risk factor of neurodegenerative diseases (3). ANG has recently been shown to mediate the production of tRNA-derived stress-induced RNA (tiRNA) (15–18), which suppress global protein translation (17). However, internal ribosome entry sequence (IRES)-mediated translation with weak eIF4G binding (19), a mechanism often used by anti-apoptosis and pro-survival genes, is not inhibited by tiRNA (17). Therefore, tiRNA reprograms protein translation in response to stress, thereby promoting cell survival (20). ANG-mediated tiRNA production is an important stress-response mechanism used by cells when they are subjected to adverse environments (21).

RNASE4, the fourth member of the superfamily, was originally co-isolated with ANG from tumor-conditioned medium (22). It has recently been shown that RNASE4 also possesses angiogenic, neurogenic, and neuroprotective activity (23). Moreover, a single nucleotide polymorphism has been shown

* This work was supported, in whole or in part, by National Institutes of Health Grants R01CA105241 and R01NS065237 (to G.-f. H.). This work was also supported by the China Scholarship Council (to J. S.).
[1] To whom correspondence may be addressed: Institute of Environmental Medicine, Zhejiang University School of Medicine, 866 Yuhangtang Rd., Hangzhou 310058, China. Tel.: 86-57188208008; Fax: 86-57188208163; E-mail: zpxu@zju.edu.cn.
[2] To whom correspondence may be addressed: Molecular Oncology Research Institute, Tufts Medical Center, 800 Washington St., Boston, MA 02111. Tel.: 617-636-4776; Fax: 617-636-9230; E-mail: ghu@tuftsmedicalcenter.org.
[3] The abbreviations used are: ANG, angiogenin; 3C, chromatin conformation capture; CAGE, cap-analysis of gene expression; CTCF, CCCTC binding factor; DAVID, Database for Annotation, Visualization, and Integrated Discovery; ENCODE, Encyclopedia of DNA Elements; Pol II, RNA polymerase II; Pol III, RNA polymerase III; RNASE4, ribonuclease 4; Pr-L, promoter-L, liver-specific promoter; Pr-U, promoter-U, universal promoter; TF, transcription factor; tiRNA, tRNA-derived stress-induced RNA; TSS, transcription start site; qRT, quantitative real-time.

to be associated in amyotrophic lateral sclerosis patients (23), and supplementary therapy with recombinant RNASE4 protein is beneficial to amyotrophic lateral sclerosis model mice (23) as is ANG (24).

These early results underscore the importance of understanding the regulatory mechanisms of *ANG* and *RNASE4* transcription so that their expression and/or activity can be potentially manipulated for therapeutic applications in both cancers and neurodegenerative diseases. Mouse *Ang1* and *Rnase4* genes have been reported to contain two non-coding exons followed by two distinct exons encoding Ang1 and Rnase4, respectively (25). The two non-coding exons are preceded by two promoters that control liver-specific and tissue-specific expression. As a consequence of this unique gene structure, *RNASE4* and *ANG* are often co-expressed (26). Human *ANG* and *RNASE4* locus has a similar arrangement to the mouse counterpart (23). Transcripts of both *ANG* and *RNASE4*, having the same 5′-UTR that contains either exon I or exon II, but not both, have been identified (23, 27). These data suggest that human *ANG* and *RNASE4* share the same genetic regions with promoter activities and are co-regulated (23, 25). In an attempt to understand the molecular mechanism by which *ANG* and *RNASE4* transcription is regulated, we used bioinformatics analyses of the data sets released from the Encyclopedia of DNA Elements (ENCODE) project to discover functional elements in the *ANG* and *RNASE4* locus. These *in silico*-discovered elements were then verified and defined experimentally by means of luciferase reporter, RNAi knockdown, and chromatin conformation capture (3-C) assays. This combined bioinformatics and experimental approach revealed a unique mechanism of transcriptional regulation at the *ANG* and *RNASE4* locus. Our data indicate that the transcriptional activity of the *ANG* and *RNASE4* promoter is influenced by RNA polymerase III (Pol III) elements and could be differentially regulated by an intragenic CCCTC binding factor (CTCF)-dependent chromatin loop.

EXPERIMENTAL PROCEDURES

Data Sets and in Silico Analyses—Human genome sequence (human species genomic assembly version, GRCh37/hg19) was downloaded from UCSC Genome Bioinformatics). The chromatin states were characterized by ChromHMM software v1.06 and annotated on UCSC human genome track. Transcription start site (TSS) data were collected from different available resources by extracting full-length cDNA sequences or deep CAGE tag data (DBTSS, FANTOM3, FANTOM4) and analyzed by Genomatix software suite (TFs were extracted from ENCODE data sets using Genomatix software suite. Function annotations of the putative TF were carried out with Database for Annotation, Visualization, and Integrated Discovery (DAVID) software.

Promoter Constructs—A 2-kb DNA fragment of human chromosome 14 from position 21,150,940 to 21,152,939 was amplified by PCR from LNCaP genomic DNA and cloned into the BglII and HindIII site of pGL3-B. The primer sequences were: forward, 5′-GAAGATCTGGAAGAGCCGAGATTGGGAGGG-3′, and reverse, 5′-CCCAAGCTTAGGAGCAGGAGTGTGAACCTACC-3′. This fragment corresponds to positions −1396 to +604 in relevance of the TSS (position 1). Serial deletion constructs were prepared by PCR using the full-length construct as the template. All constructs were sequence confirmed.

Cell Culture, Transfection, and Reporter Assays—Prostate cancer cell lines (LNCaP, PC-3, and DU145) were maintained in RPMI 1640 medium + 10% FBS. U87MG glioblastoma and human embryonic kidney 293T cells were maintained in DMEM + 10% FBS. Transfections were carried out in the presence of Lipofectamine® 2000 in 70% confluent cells. pRL-TK plasmid expressing *Renilla* luciferase (0.016 μg) was co-transfected as an internal control for transfection efficiency with various target constructs expressing firefly luciferase (0.8 μg). Luciferase activities were measured by the Dual-Luciferase® Reporter Assay 24 h after transfection. The firefly luciferase activity was normalized to the *Renilla* luciferase in each sample. The promoter activity of each construct was normalized to that of the control plasmid pGL3-B.

Chromatin Immunoprecipitation (ChIP)—Cells were cross-linked with 1% formaldehyde for 10 min at 37 °C and quenched with 0.125 M glycine. Cell pellets were collected and resuspended in ChIP lysis buffer (50 mM Tris, pH 8.1, 1% SDS, 10 mM EDTA). After sonication to generate DNA fragments of 300–1000 bp, the lysates were cleared by centrifugation and diluted 10-fold with ChIP dilution buffer (16.7 mM Tris, pH 8.1, 0.01% SDS, 1.1% Triton X-100, 1.2 mM EDTA, 16.7 mM NaCl). After preclearing with salmon sperm DNA/protein G-agarose at 4 °C for 1 h, the samples were incubated with 5 μg of CTCF IgG or control non-immune IgG overnight at 4 °C. The immunocomplexes were collected with protein-G-agarose, eluted, and de-cross–linked at 65 °C. After incubation with RNase A and proteinase K, DNA was extracted and examined by quantitative PCR with the primers for site A (forward, 5′-ACAGCATTGGCACCTCCTGCAA-3′; reverse, 5′-TGCCTGGTGCCAGAATCCCAG-3′) and site B (forward, 5′-TCAAGACTGGAGGTGGACTCAC-3′; reverse, 5′-TCAAGACTGGAGGTGGACTCAC-3′).

RNAi—Lentiviral particles vectors (GIPZ) encoding *ANG* and *RNASE4* shRNA were purchased from Open Biosystems. The sequences of the two *ANG* shRNA used in this study are: E4, 5′-ATGTTTGACAACATGTTTAATA-3′; E7, 5′-CAACGTTGTTGTTGCTTGTGAA-3′. That for RNASE4 are: D10, 5′-CCCTAGTAAGTCAAAGTACTA-3′; M2, 5′-CACCACCAATATCCAATGCAA-3′. The shRNA for CTCF (5′-GGACAGTGTTGACAACTAA-3′ and 5′-GGTGCAATTGAGAACATTA-3′) were gifts from Dr. Joaquin M. Espinosa of University of Colorado (28). Lentiviral particles were packaged in 293T cells with the generation II packaging plasmids (psPAX2 and pMD2.G). Cells were infected with lentiviral particles for 24 h in the presence of Polybrene (8 μg/ml, Millipore). The medium was replaced with complete growth medium and incubated for 24 h and then selected for 4 days with 1 μg/ml puromycin.

RT-PCR—Total cellular RNA was isolated using TRIzol reagent and reverse-transcribed (1 μg) to cDNA with random and oligo(dT)18 primers by M-MLV reverse transcriptase. cDNAs were amplified and quantified in DNA Engine Opticon 2. The primers set are as follows. ANG forward, 5′-GTTGGAAGAGATGGTGATGG-3′; reverse, 5′-CATAGTGCTGGGTCAGG-

AAG-3′; RNASE4 forward, 5′-AGAAGCGGGTGAGAAA-CAA-3′; reverse, (5′-AGTAGCGATCACTGCCACCT-3′); CTCF forward, 5′-CAGTGGAGAATTGGTTCGGCA-3′; reverse, 5′-CTGGCGTAATCGCACATGGA-3′; GAPDH forward, 5′-TGAACGGGAAGCTCACTGG-3′; reverse, 5′-TCCACC-ACCCTGTTGCTGTA-3′.

Chromosome Conformation Capture (3C)—A total of 1×10^7 cells were trypsinized and resuspended in 10 ml of medium and cross-linked with 2% formaldehyde for 10 m at room temperature. Cross-linking was quenched by 0.125 M glycine. After washing with cold PBS, cells were lysed in 3C lysis buffer (10 mM Tris, pH 8.0, 10 mM NaCl, 0.2% Nonidet P-40) for 10 min on ice. Nuclei were pelleted by centrifugation at 1800 rpm for 5 m at 4 °C and resuspended with 1.2× restriction enzyme buffer containing 0.3% SDS. After a 1-h incubation at 37 °C, Triton X-100 was added to 2% and incubated for 1 h at 37 °C. Chromatin was then digested by 400 units of StuI overnight at 37 °C. Digestion was stopped by the addition of SDS to 1.6% followed by heated inactivation at 65 °C for 20 min. The digested chromatin was diluted to 6.125 ml by 1.15 × 3C ligation buffer (660 mM Tris, pH 7.5, 50 mM $MgCl_2$, 10 mM DTT, and 1 mM ATP). Triton X-100 was then added to a final concentration of 1% and incubated for 1 h at 37 °C with gentle shaking. The chromatin was then ligated by incubating with 2000 units of T4 DNA ligase overnight at 16 °C. After overnight incubation with 10 μg/ml proteinase K at 65 °C to reverse the cross-links, ligated DNA was extracted and examined by PCR. The sequences of primers are as follows: 1R, 5′-ACCCACGTGATCGTGGATGAAC-3′; 2F, 5′-AGAAAGAGAGCCCACTTTGCTCACC-3′; 4F, 5′-GCTGTGATTGTTGGCTTTGCAAGG-3′; 4R, 5′-GACACC-GTGGTCTAAAAGACTGAGG-3′; 5F, 5′-GGAGTGACGG-CCAGATGGCA-3′.

RESULTS

Chromatin State Segmentation of ANG and RNASE4 Gene Locus—The human *ANG* and *RNASE4* genes are located on chromosome 14q11.2 and have a unique arrangement in which they share the same promoter regions and 5′-UTR followed by two distinct exons encoding the two proteins (23, 25). Promoter sharing is one of the four known co-regulatory mechanisms that ensure multiple genes with similar activities or involved in the same pathways are co-regulated. Among the 24 known gene pairs that share the same promoters in the human genome (29), *ANG* and *RNASE4* have the highest co-efficiency ($r = 0.77$) of co-expression (29), indicating that they have a similar biological activity. Indeed, we have found that besides the ribonucleolytic activities, ANG and RNASE4 both have angiogenic, neurogenic, and neuroprotective activities (23). To understand the regulatory mechanisms of *ANG* and *RNASE4* expression, we employed ChromHMM, a chromatin-state discovery and characterization software (ChromHMM), to reveal the chromatin state of the human *ANG* and *RNASE4* gene locus (chr14: 21,150,000–21,170,000, genome assembly version GRCh37/hg19 (30)). We identified three regulatory regions at this locus from data released by the ENCODE project: an active promoter region (red) from position 21,150,000 to 21,153,000 and two insulators (blue) from 21,159,364 to 12,159,383 and from 21,166,070 to 21,166,089 (Fig. 1*A*). It is notable that the two insulators are located in the two introns flanking the *ANG* coding exon.

Bioinformatics Analysis of the TSS—We next used the Genomatix software suite to predict TSS of *ANG* and *RNASE4* genes from cap-analysis of gene expression (CAGE) databases. A total of 113 CAGE tags were identified across the entire gene locus, clustered in two regions (Fig. 1*B*). Seven tags were located at position 21,156,940 before exon II, which occurs only in liver cells, indicating a liver-specific promoter (Promoter-L) at this region. In a 700-bp region from 21,152,300 to 21,153,000 that covers exon I and the flanking regions, we identified a total of 106 tags at 44 different positions from all tissue types including liver, intestine, cecum, colon, lung, kidney, frontal lobe, heart, adipose, and embryo. We, therefore, named this region promoter-U (Pr-U) indicating a universal promoter. Among the 106 CAGE tags, 21 occur at position 21,152,776. We have also identified a CpG island from position 21,152,484 to 21,152,740. These data suggest that *ANG* and *RNASE4* belong to a gene class with a "broad" TSS (31) that can initiate transcription in a broader region.

Putative TFs on Pr-U of ANG and RNASE4 Gene Locus—In silico analyses using the Genomatix software suite revealed a total of 26 TFs that could potentially bind to Pr-U of the *ANG* and *RNASE4* gene (Table 1). Significantly, eight of them belong to the nuclear receptor superfamily. A more detailed analysis on TFs was carried out with data available from the ENCODE project. Cscan analyses (32) identified 63 putative TFs. Among these, 6 belong to the nuclear receptor superfamily (Table 1). Preferential enrichment of the nuclear receptor class of TFs on *ANG* and *RNASE4* promoter is consistent with known functions of ANG in hormone-regulated prostate (5, 33–35) and breast (36, 37) cancer.

To reveal other potential biological activities of ANG and RNASE4, we carried out pathway annotations by DAVID bioinformatics tools. Table 2 lists the top 10 pathways identified from the Kyoto Encyclopedia of Genes and Genomes (KEGG) (38) and BioCarta databases. TFs that are enriched in the *ANG* and *RNASE4* promoter are related in pathways in cancer, particularly in prostate, pancreatic, thyroid, bladder, and non-small cell lung cancers, and in chronic myeloid leukemia (Table 2). In addition, cell cycle and Huntington disease pathways are also significantly correlated. These findings are consistent with the roles of ANG and RNASE4 in cancers and neurodegenerative diseases (3).

Characterizations of ANG and RNASE4 Promoters—A luciferase reporter assay system was used to confirm that Pr-U indeed has promoter activity and to define the minimum promoter sequence. A 2-kb region from positions 21,150,940 to 21,152,939, referred as 1–2000 in luciferase assays, was cloned into pGL3-B reporter vector, and the promoter activity was examined in 5 cell lines. Fig. 2*A* shows that this 2-kb fragment, which was named Pr-U, has prominent activity in all five cell lines including prostate cancer cell lines PC-3 and DU145, glioblastoma cell line U87MG, human embryonic kidney cells HEK293T, and hepatocellular carcinoma cells HepG2. However, promoter-L (Pr-L) (from position 21,154,000 to 21,156,000) has activity only in HepG2 cells.

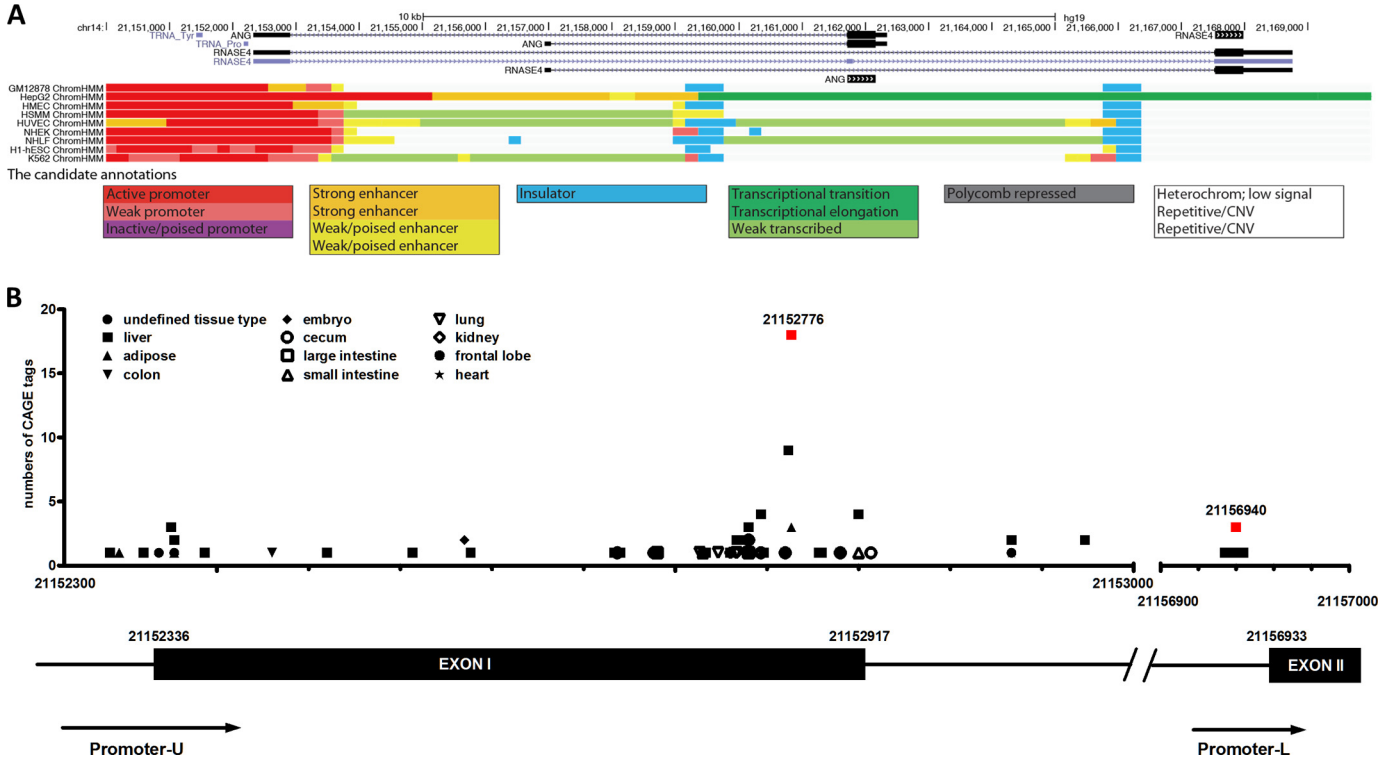

FIGURE 1. **Bioinformatics analyses of ANG and RNASE4 gene locus.** *A*, chromatin state annotation of *ANG* and *RNASE4* gene locus. A common set of chromatin state annotation across nine cell types were computed by integrating ChIP-seq data from nine factors (CTCF, H3K27ac, H3K27me3, H3K36me3, H3K4me1, H3K4me2, H3K4me3, H3K9ac, H4K20me1). Active promoter was colored with *red*, and two insulators were colored with *blue*. CNV, copy number variation. *B*, bioinformatics analysis of the transcription start site. The Genomatix software suite was used to identify CAGE tags in the entire region of the gene locus from three databases, DBTSS, FANTOM3, and FANTOM4. *x axis*, positions of the *ANG* and *RNASE4* promoter region on chromosome 14. *y axis*, total numbers of CAGE tags identified in different tissues for each particular start site. The most common start site in the cluster is position 21,152,776. The *red squares* mark the position of active promoter regions. The *diagram at the bottom* is a linear presentation of the two promoters (Pr-U and Pr-L) and the two exons (Exon 1 and 2).

We next made a series of deletion mutants of Pr-U and measured their reporter activities in DU145 cells (Fig. 2*B*). For deletion constructs from the 5′ end, after an initial decrease of activity (FU-1), deletions gradually increased activity (FU-1 to FU-6). The maximum activity was observed in FU-6. However, further deletion resulted in activity loss as shown in constructs FU-7 to FU-9. Among the series of deletion constructs proceeding from the 3′ end, no significant promoter activity was observed from FD-1 to FD-6. However, FD-7 that retains only 200 bp of the 5′ sequence had the highest promoter activity among all the constructs including the full-length construct. The first 100 bp of the 5′ sequence (FD-8) also has a significant promoter activity. Very similar results were obtained in PC-3 cells (Fig. 3).

RNA Pol III-occupied Elements Affect Pol II Promoter Activity—These data indicate that two promoters exist in Pr-U. The first (Pr-1) is located at 1–200 and the second (Pr-2) is located at 1,750–2,000. It is also obvious that inhibitory elements exist between 201 and 1200. We confirmed that internal sections between 201 and 1432 have no promoter activities (Fig. 2*C*). To identify the nature of these inhibitory elements, we re-evaluated this region by bioinformatics analyses of the ENCODE project data and found that two tRNA genes ($tRNA^{Tyr}$ and $tRNA^{Pro}$), located at 21,151,432–21,151,520 and 21,152,175–21,152,246, respectively, were fully loaded with Pol III transcription machinery including Pol III, TFIIIB, and TFIIIC (Fig. 4). They are, therefore, referred to as Pol III elements.

The effect of these Pol III elements on Pol II transcription was examined by reporter assays (Fig. 5*A*). Insertion of the $tRNA^{Tyr}$ element downstream of Pr-1 in forward orientation decreased the promoter activity from 50.1 ± 7.9 in P-1 to 9.19 ± 1.99 in P-2 ($p < 0.0001$). However, insertion in reverse orientation at the same position had no effect. The activity of P-3 is 42.3 ± 6.8, not significantly different from that of P-1 ($p = 0.26$). Similarly, the $tRNA^{Tyr}$ element also suppresses the activity of Pr-2. Construct P-5 has an activity of 5.6 ± 0.1, representing a 6-fold decrease from that of P-4 (34.1 ± 5.6, $p = 0.002$). Again, insertion in reverse orientation had no effect on Pr-2. P-6 has an activity of 32.3 ± 4.6, which is the same as that of P-4 ($p = 0.67$). $tRNA^{Pro}$ element, the 2nd Pol III element found in this region, also suppresses transcription as shown in P-7. Insertion of this element together with Pr-2, downstream of Pr-1, decreased the activity from 50.1 ± 7.9 in P-1 to 31.6 ± 3.0 in P-7 ($p = 0.002$). The activity of P-7 was the same as that of P-4, indicating that Pr-1 was completely suppressed by $tRNA^{Pro}$.

Insertion of $tRNA^{Tyr}$ element upstream of Pr-1 in forward orientation enhanced the promoter activity from 50.1 ± 7.9 in P-1 to 74.1 ± 12.0 in P-8 ($p = 0.02$) (Fig. 5*B*). P-9, which has $tRNA^{Tyr}$ element inserted in reverse orientation upstream of Pr-1, had the same activity as that of P-1 ($p = 0.83$), indicating that the enhancer activity of $tRNA^{Tyr}$ element is orientation-dependent. However, when we placed the $tRNA^{Tyr}$ element, in both forward and reverse orientations, upstream of Pr-2 that already had the $tRNA^{Pro}$ element, no further enhancement of

TABLE 1

TFs associated with *ANG* and *RANSE4* Pr-U

Symbols for of the nuclear receptor family are indicated with italics and boldface type.

Symbol	Gene name
***In silico* prediction**	
AR	Androgen receptor
ATF4	Activating transcription factor4 (tax-responsive enhancer element B67)
BHLHE40	Basic helix-loop-helix family, member e40
CREB1	cAMP-responsive element-binding protein 1
EGR1	Early growth response 1
ESR1	Estrogen receptor 1
FOXO1	Forkhead box O1
HIF1α	Hypoxia-inducible factor 1, α-subunit (basic helix-loop-helix transcription factor)
HNF1α	Hepatocyte nuclear factor 1α
JUN	jun oncogene
LHX1	LIM homeobox 1
LYL1	Lymphoblastic leukemia-derived sequence 1
MYC	v-myc myelocytomatosis viral oncogene homolog (avian)
NANOG	Nanog homeobox
NFKB1	Nuclear factor of κ light polypeptide gene enhancer in B-cells 1
NR3C2	Nuclear receptor subfamily 3, group C, member 2 (mineralocorticoid receptor)
PBX1	Pre-B-cell leukemia homeobox 1
PGR	Progesterone receptor
POU5F1	POU class 5 homeobox 1
PPARα	Peroxisome proliferator-activated receptor α
PPARγ	Peroxisome proliferator-activated receptor γ
STAT3	Signal transducer and activator of transcription3 (acute-phase response factor)
TCF3	Transcription factor3 (E2A immunoglobulin enhancer binding factors E12/E47)
TP53	Tumor protein p53
VDR	VitaminD (1,25- dihydroxyvitamin D3) receptor
XBP1	X-box binding protein 1
Cscan	
TFAP2A	Transcription factor AP-2α (activating enhancer binding protein 2α)
TFAP2C	Transcription factor AP-2γ (activating enhancer binding protein 2γ)
SMARCC2	SWI/SNF related, matrix associated, actin dependent regulator of chromatin, subfamily c, member 2
BATF	Basic leucine zipper transcription factor, ATF-like
BCL3	B-cell CLL/lymphoma 3
BCLAF1	BCL2-associated transcription factor 1
BDP1	Subunit of RNA polymerase III transcription initiation factor IIIB
BRCA1	Breast cancer 1, early onset
BRF1	BRF1 homolog, subunit of RNA polymerase III transcription initiation factor IIIB
FOS	FBJ murine osteosarcoma viral oncogene homolog
CEBPB	CCAAT/enhancer binding protein (C/EBP), beta
CHD2	Chromodomain helicase DNA binding protein 2
E2F1	E2F transcription factor 1
E2F4	E2F transcription factor 4, p107/p130 binding
E2F6	E2F transcription factor 6
EBF1	Early B-cell factor 1
ELF1	E74-like factor 1 (ets domain transcription factor)
ETS1	v-ets erythroblastosis virus E26 oncogene homolog 1
FOSL2	FOS-like antigen 2
FOXA1	Forkhead box A1
FOXA2	Forkhead box A2
GATA2	GATA-binding protein 2
GATA3	GATA-binding protein 3
NR3C1	Nuclear receptor subfamily 3, group C, member 1 (glucocorticoid receptor)
GTF2F1	General transcription factor IIF, polypeptide 1, 74 kDa
HDAC2	Histone deacetylase 2
HEY1	Hairy/enhancer-of-split related with YRPW motif 1
HNF4A	Hepatocyte nuclear factor 4α
HNF4G	Hepatocyte nuclear factor 4γ
HSF1	Heat shock transcription factor 1
IRF4	Interferon regulatory factor 4
JunD	jun D proto-oncogene
TRIM28	Tripartite motif containing 28
MAFF	v-maf musculoaponeurotic fibrosarcoma oncogene homolog F
MAFK	v-maf musculoaponeurotic fibrosarcoma oncogene homolog K
NFKB1	Nuclear factor of κ light polypeptide gene enhancer in B-cells 1
EP300	E1A-binding protein p300
PAX5	Paired box 5
PBX3	Pre B cell leukemia homeobox 3
PPARGC1A	Peroxisome proliferator-activated receptor γ, coactivator 1α
RAD21	RAD21 homolog
RB1	Retinoblastoma 1
RFX5	Regulatory factor X, 5 (influences HLA class II expression)
POLR3A	Polymerase (RNA) III (DNA directed) polypeptide A, 155kDa
RXRA	Retinoid X receptor α
SIN3A	SIN3 transcription regulator homolog A (yeast)
SMC3	Structural maintenance of chromosomes 3
SP1	Sp1 transcription factor
SREBF2	Sterol regulatory element binding transcription factor 2
SRF	Serum response factor (c-fos serum response element-binding transcription factor)

TABLE 1 —*continued*

Symbol	Gene name
STAT1	Signal transducer and activator of transcription 1, 91 kDa
TAF1	TAF1 RNA polymerase II, TATA box binding protein (TBP)-associated factor, 250 kDa
TAL1	T-cell acute lymphocytic leukemia 1
TBP	TATA box binding protein
TCF4	Transcription factor 4
GTF3C2	General transcription factor IIIC, polypeptide 2, beta 110kDa
USF1	Upstream transcription factor 1
USF2	Upstream transcription factor 2, c-fos interacting
YY1	YY1 transcription factor
ZBTB33	Zinc finger and BTB domain containing 33
ZEB1	Zinc finger E-box binding homeobox 1
ZNF143	Zinc finger protein 143
ZNF263	Zinc finger protein 263

TABLE 2
Pathway annotation by DAVID

Pathways	Genes	*p* Value
KEGG database		
Pathways in cancer	E2F1, AR, RXRA, PPARG, TP53, FOXO1, NFKB1, RB1, STAT1, STAT3, FOS, HDAC2, EP300, HIF1A, ETS1, JUN, MYC	2.24E-09
Prostate cancer	E2F1, AR, ATF4, EP300, CREB1, TP53, FOXO1, NFKB1, RB1	4.65E-07
Cell cycle	E2F1, RAD21, EP300, HDAC2, E2F4, TP53, RB1, MYC, SMC3	6.24E-06
Huntington disease	SIN3A, EP300, HDAC2, SP1, CREB1, PPARG, TP53, TBP, PPARGC1A	8.87E-05
Pancreatic cancer	E2F1, TP53, NFKB1, RB1, STAT1, STAT3	2.80E-04
Chronic myeloid leukemia	E2F1, HDAC2, TP53, NFKB1, RB1, MYC	3.39E-04
Small cell lung cancer	E2F1, RXRA, TP53, NFKB1, RB1, MYC	5.74E-04
Maturity onset diabetes of young	HNF1A, HNF4A, FOXA2, HNF4G	0.0011
Thyroid cancer	RXRA, PPARG, TP53, MYC	0.0016
Adipocytokine signaling pathway	PPARA, RXRA, NFKB1, PPARGC1A, STAT3	0.0021
Bladder cancer	E2F1, TP53, RB1, MYC	0.0048
MAPK signaling	FOS, ATF4, JUN, JUND, TP53, NFKB1, SRF, MYC	0.0056
Non-small cell lung cancer	E2F1, RXRA, TP53, RB1	0.0097
BioCarta database		
METS effect on macrophage differentiation	E2F1, FOS, SIN3A, HDAC2, E2F4, ETS1, JUN	3.22E-06
CARM1 and regulation of the estrogen receptor	EP300, HDAC2, GTF2F1, ESR1, TBP, PPARGC1A, BRCA1	5.82E-05
Mechanism of gene regulation by peroxisome proliferators via PPAR	PPARα, EP300, SP1, JUN, RXRA, RB1, PPARγC1A	0.0012
Role of PPAR-γ coactivators in obesity and thermogenesis	EP300, RXRA, PPARG, PPARGC1A	0.0019
Oxidative stress-induced gene expression via Nrf2	MAFF, FOS, JUN, CREB1, MAFK	0.0019
IL-6 signaling pathway	FOS, CEBPB, JUN, SRF, STAT3	0.0019
PDGF signaling pathway	FOS, JUN, STAT1, SRF, STAT3	0.0056
EGF signaling pathway	FOS, JUN, STAT1, SRF, STAT3	0.0064
Human cytomegalovirus and map kinase pathways	SP1, CREB1, NFKB1, RB1	0.0072
Hypoxia-inducible factor in the cardiovascular system	HIF1A, EP300, JUN, CREB1	0.0088

transcription activity was observed (P-10 and P-11 *versus* P-4). Fig. 2*B* has already shown that the $tRNA^{Pro}$ element enhances Pr-2 activity (FU-6 *versus* FU-7). Thus, it is clear that when these Pol III elements are located upstream of Pol II promoters in forward orientation, they enhance Pol II transcription. The existence of multiple Pol III elements does not amplify the enhancement activity. Identical results were obtained in three other cell lines including PC-3 human prostate cancer (Fig. 6*A*), 293T human embryonic kidney (Fig. 6*B*), and U87MG human glioblastoma (Fig. 6*C*) cells. Taken together, these results indicate that $tRNA^{Tyr}$ and $tRNA^{Pro}$ elements located upstream of the *ANG* and *RNASE4* promoter can affect Pol II gene transcription in a position- and orientation-dependent manner.

To know whether the observation that Pol III elements interfere with Pol II transcription is applicable to other promoters, we examined the effect of $tRNA^{Tyr}$ element on SV40 promoter activity. Fig. 5*C* shows that insertion of $tRNA^{Tyr}$ element in forward orientation downstream of the SV40 promoter decreases the activity to 37 ± 10% (P-13) of that of control (P-12) ($p < 0.002$). Insertion in reverse orientation (P-14) had no significant effect (89 ± 2%, $p = 0.24$). Insertion upstream of SV40 promoter in forward orientation enhanced activity by 2.6-fold (P-15, 259 ± 20%, $p < 0.0001$) but had no significant effect if inserted in reverse orientation (P-16, 122 ± 18%, $p = 0.14$). These results confirmed the position- and orientation-dependent manner of Pol III elements in either enhancing or inhibiting Pol II activity. To our knowledge this is the first experimental report that Pol III elements regulate transcription of Pol II genes.

Formation of a CTCF-dependent Chromatin Loop between the Two Introns Flanking the ANG Coding Exon—Another distinct feature of the *ANG* and *RNASE4* gene locus is that there are two insulators located in the introns flanking the *ANG* coding exon (Fig. 1*A*). We have identified two CTCF binding sites within the two insulators by CTCF ChIP-seq data from the ENCODE project in five cell lines (Fig. 7*A*). CTCF is a ubiquitously expressed and highly conserved 11-zinc finger protein and has been implicated in diverse cellular processes (39). CTCF has been shown to both positively and negatively regulate gene expression (40, 41). It not only interacts with the initiation and elongation complex but also affects transcript splicing (42, 43), thereby affecting overall transcription levels (44). Moreover, CTCF has been recognized as a master organizer of genomic spatial structure by mediating long range chromosomal interactions through looping (40). The sequences of the two CTCF binding sites on *ANG* and *RNASE4* locus were both

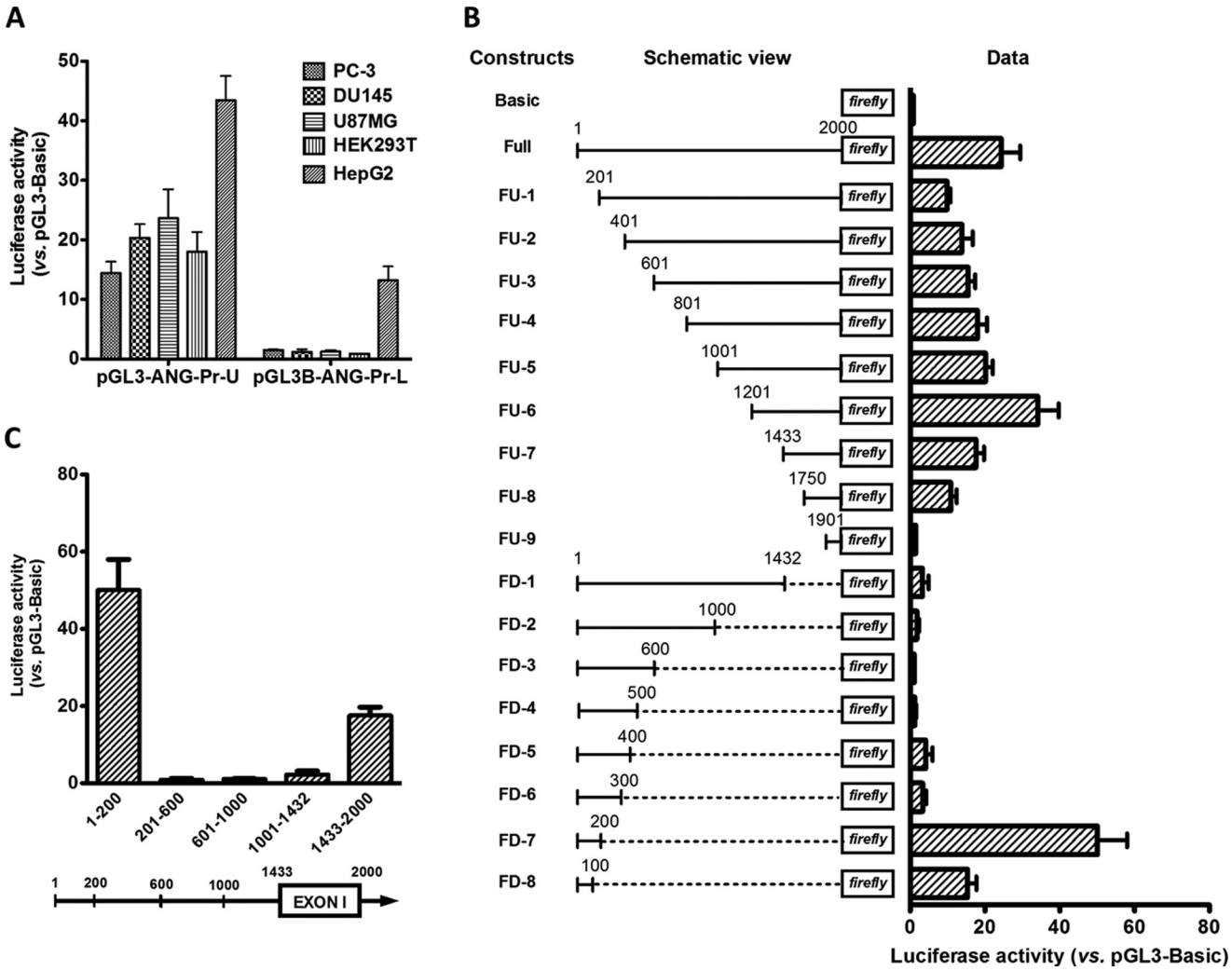

FIGURE 2. **Characterization of human *ANG* and *RNASE4* promoters.** *A*, activity of Pr-U and Pr-L in driving luciferase reporter gene expression in various cell lines. Data shown are the means ± S.D. of six independent experiments. *B*, luciferase reporter activity of serial deletion mutants of Pr-U. The *left panel* is the schematic views of the deletion constructs. The *bar graphs at the right* are luciferase activities of these constructs normalized to pGL3-B control plasmid. Data shown are the means ± S.D. of four independent experiments. *C*, promoter activity of internal sections of Pr-U in luciferase reporter assay. The five fragments with positions as marked were cloned into pGL3-B, and the promoter activities in driving luciferase reporter gene expression were measured in DU145 cells. Data shown are the means ± S.D. of four independent experiments.

85% identical to the consensus CTCF binding sequence (45) (Fig. 7*B*).

ChIP was carried out to examine the binding of CTCF to the two sites in control and CTCF knockdown cells. Lentivirus-mediated shRNA constructs efficiently knocked down both mRNA and protein of CTCF (Fig. 8*A*). ChIP combined with normal PCR (Fig. 8*B*) and quantitative PCR (Fig. 8*C*) show that binding of CTCF to both sites diminished in CTCF knockdown cells, demonstrating that CTCF is indeed bound at the two consensus sites located at the two introns flanking the *ANG* coding exon.

CTCF is known to mediate the formation of chromatin loops facilitating transcription regulation (40). We, therefore, examined such a possibility in the *ANG* and *RNASE4* locus by 3C analysis (46). Fig. 9*A* is a schematic view of dynamic spatial organization of this region. The *arrows* show the primers used for PCR amplification in this 3C experiment. *Vertical lines* mark the restriction enzyme StuI sites. If such a loop forms, after cross-linking, StuI digestion, and T4 ligation, one would expect a PCR product to be produced by primer sets 2F/4R and 5F/1R. However, primer sets 2F/1R and 5F/4R will generate amplicons regardless of cross-linking as far as the products were ligated (self ligation). Fig. 9*B* shows that the 3C experiments generated the results exactly as we expected, indicating an intragenic loop is indeed formed between the two CTCF binding sites. The PCR products from primer sets 2F/4R and 5F/1R were recovered, and the sequencing results confirmed the loop formation.

To confirm that formation of this chromatin loop is CTCF-dependent, we carried out a ChIP-3C experiment (Fig. 9*C*) in which chromatin was precipitated by a non-immune or a CTCF-specific IgG. Immunoprecipitated chromatin was then subjected to 3C analysis. A specific band was observed from CTCF-specific immunoprecipitated chromatin but not from control IgG immunoprecipitates. We have also performed ChIP-3C experiments in CTCF knockdown cells (Fig. 9*C*). As expected, the PCR products generated from primer sets 2F/4R and 5F/1R were undetectable in CTCF knockdown cells. Taken

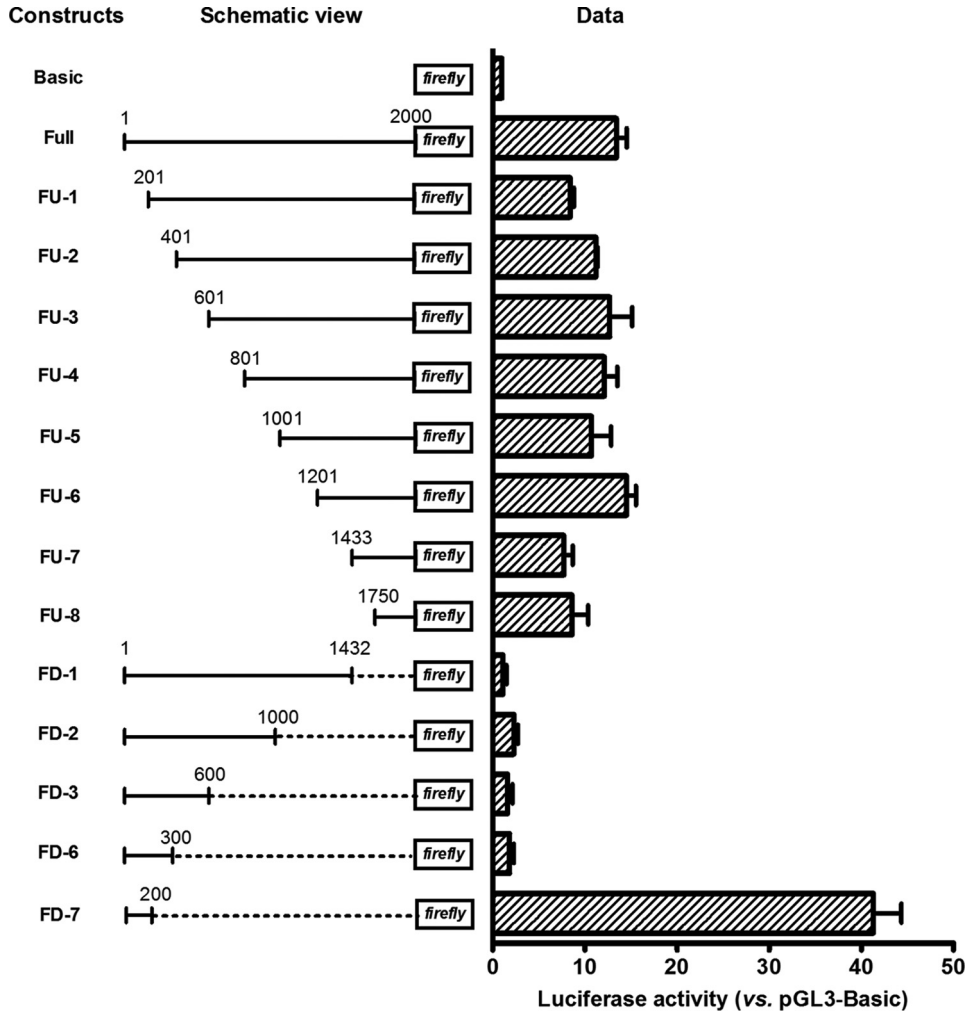

FIGURE 3. **Luciferase reporter activity of serial deletion mutants of Pr-U in PC-3 cells.** Luciferase activities of various constructs were measured by a dual luciferase reporter system with Renilla luciferase as internal control. Data shown are means ± S.D. of three independent experiments.

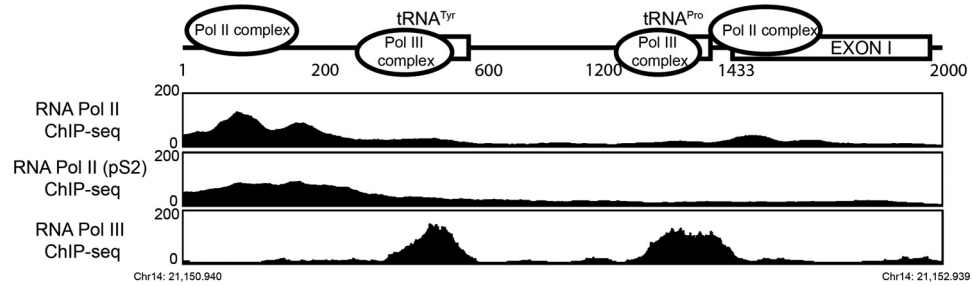

FIGURE 4. **Bioinformatics analyses of Pol II and RNA Pol III occupancy on promoter-U from the ChIP-seq data released by the ENCODE project.** The *top panel* is a schematic view of ANG and RNASE4 promoter-U region with Pol II and Pol III binding complex noted. The *bottom panels* are the enrichment of Pol II, Pol II phosphoS2 (large subunit-specific for phosphorylated C-terminal domain), and Pol III in this region.

together, these results demonstrate that CTCF mediates the formation of an intragenic chromatin loop between the two introns flanking the coding exon of ANG gene.

CTCF Influences the mRNA level of ANG and RNASE4—We next examined the effect of CTCF level on the mRNA level of *ANG* and *RNASE4*. Two shRNA constructs knocked down *CTCF* mRNA levels by 71 and 76%, respectively (Fig. 10*A*, *left*). Immunoblot analyses indicated a nearly complete loss of CTCF protein in the knockdown cells (Fig. 10*A*, *right*). *ANG* mRNA levels in the shRNA1- and shRNA2-infected cells were 55 ± 9 and 35 ± 10%, respectively, that in control cells (Fig. 10*B*). Similarly, the mRNA levels of *RNASE4* in the two CTCF knockdown cell lines were 62 ± 6 and 33 ± 4% that in control cells (Fig. 10*B*). ELISA analyses showed that secreted ANG protein levels were 1.40 ± 0.25 and 1.12 ± 0.23 pg/1000 cells/day, respectively, in the two knockdown cell lines, which is significantly lower than that in control cells (1.9 ± 0.13 pg/1000 cells/day) (Fig. 10*C*). The protein levels of RNASE4 in these cells are unknown as an ELISA method is currently unavailable. However, judging from the quantitative PCR results, it is clear that knock-

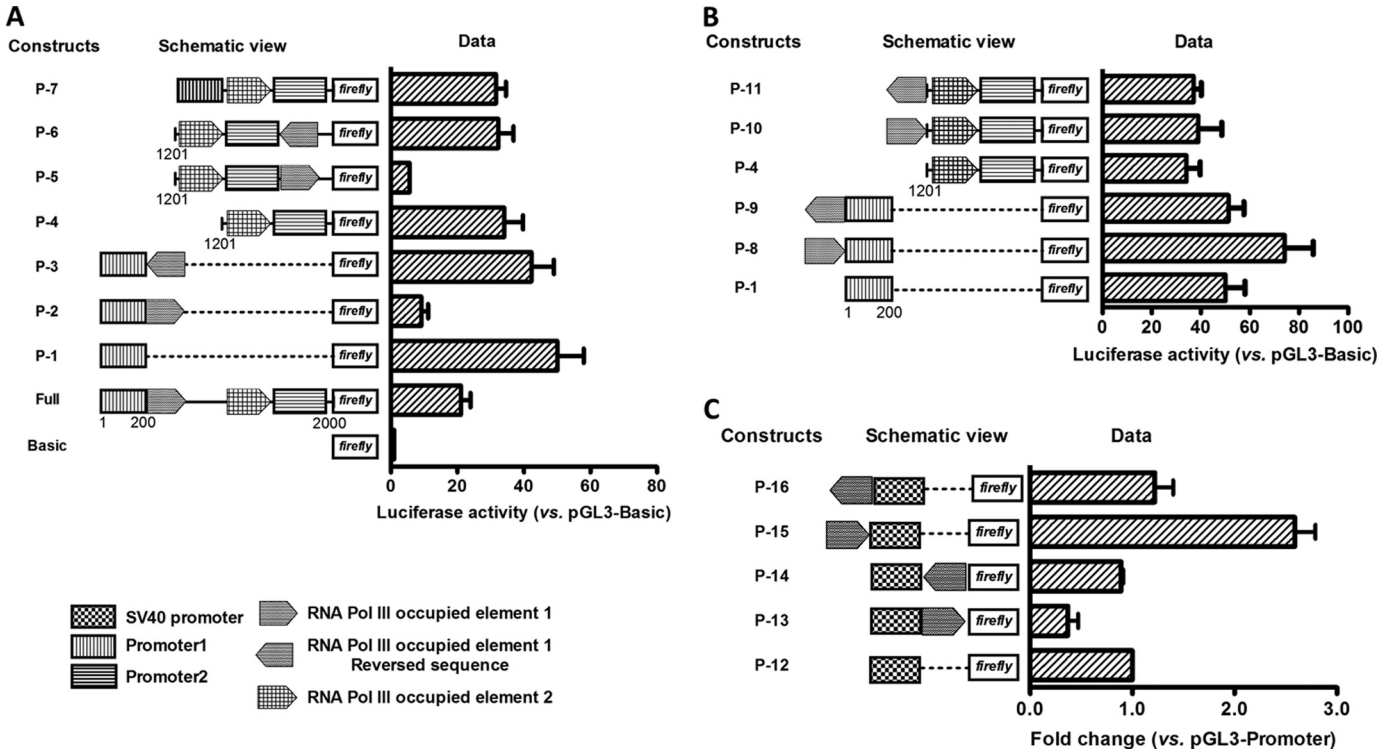

FIGURE 5. **Effect of Pol III-occupied elements on Pol II gene transcription.** *A*, inhibitory activity of the Pol III element when positioned in forward orientation downstream of Pol II promoter. The $tRNA^{Tyr}$ and $tRNA^{Pro}$ elements identified within Pr-U were cloned to various positions in both forward and reverse orientations as indicated. The luciferase activity was measured in DU145 cells. *B*, enhancive activity of Pol III elements when positioned in forward orientation at upstream of Pol II promoter. The $tRNA^{Tyr}$ element was cloned upstream of Pr-1 or Pr-2 as indicated, and reporter activity was measured as described above in *A*. *C*, effect of Pol III element on SV40 promoter activity. The $tRNA^{Tyr}$ element was cloned in to the pGL3-P constructs upstream or downstream of SV40 promoter in either forward or reverse orientation. The reporter activities of these constructs were measured by the dual luciferase system and normalized to pGL3-P. Data shown are the means ± S.D. of three independent experiments.

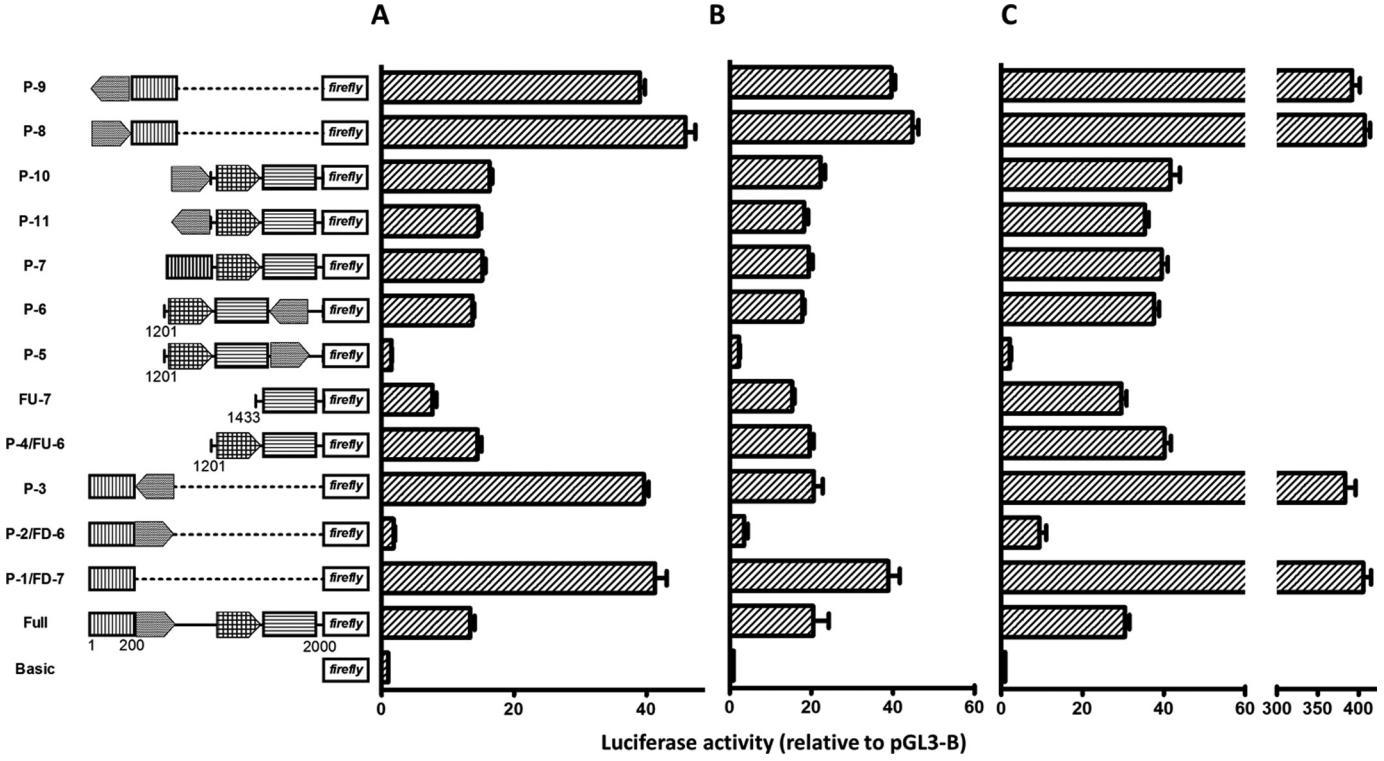

FIGURE 6. **Effect of Pol III elements on reporter activities of Pr-1 and Pr-2.** Pol III elements were inserted upstream or downstream of Pr-1 or Pr-2, and the reporter activities of each construct were examined by a dual luciferase reporter system in PC-3 (*A*), 293T (*B*), and U87MG (*C*) cells. Data shown are the means ± S.D. of three independent experiments.

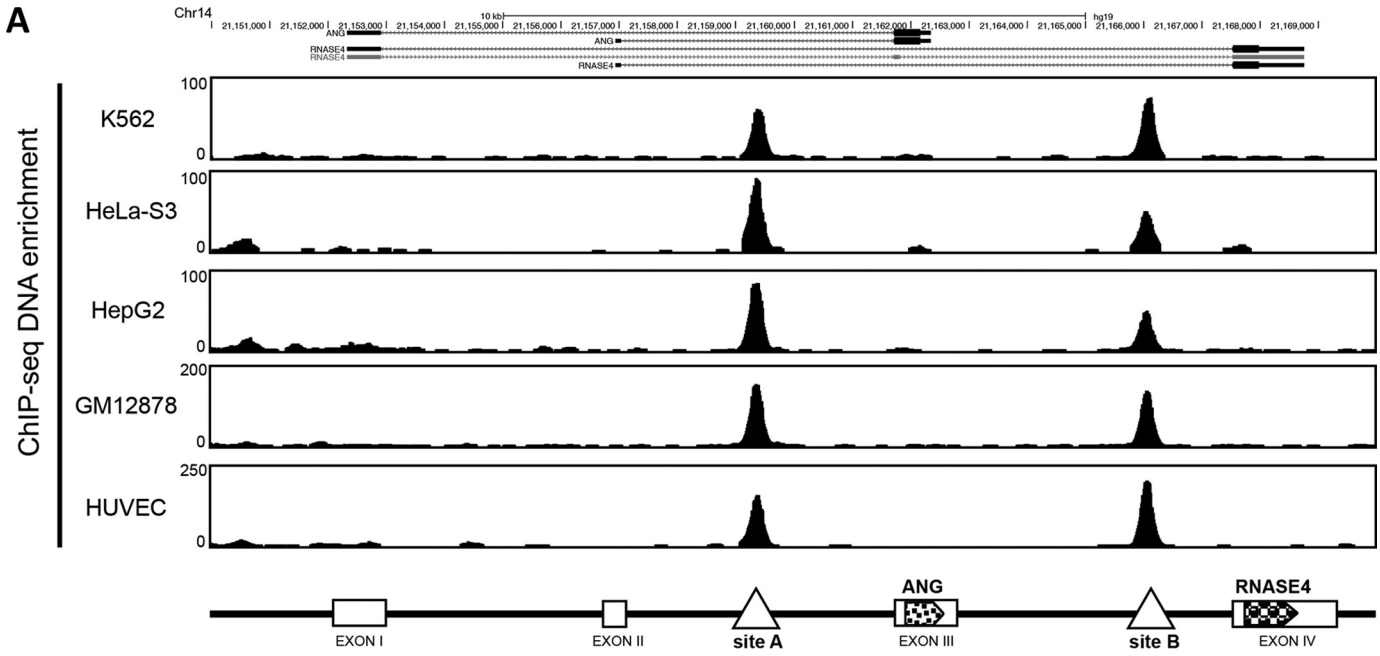

B

Name	Sequence
CTCF consensus motif	- - - - C C G C N - G G N G G C A G - -
Human Site B	21,166,070- G T G A C G G C C A G A T G G C A G C A -21,166,089
Human Site A	21,159,364- A G A G T C G T T A G G T G G C A G T G -21,159,383
Consensus	R K R R C C G C Y A G G T G G C A G Y R

FIGURE 7. **Identification of CTCF binding sites in ANG and RNASE4 gene locus.** *A*, bioinformatics analyses of CTCF occupancy in five cell lines from the ChIP-seq data released by the ENCODE project. The *top panel* shows the enrichment of CTCF in the two introns flanking the ANG coding exon. The *bottom panel* is a schematic view of CTCF binding sites in this gene locus. *B*, consensus CTCF binding motif identified in the two CTCF binding sites.

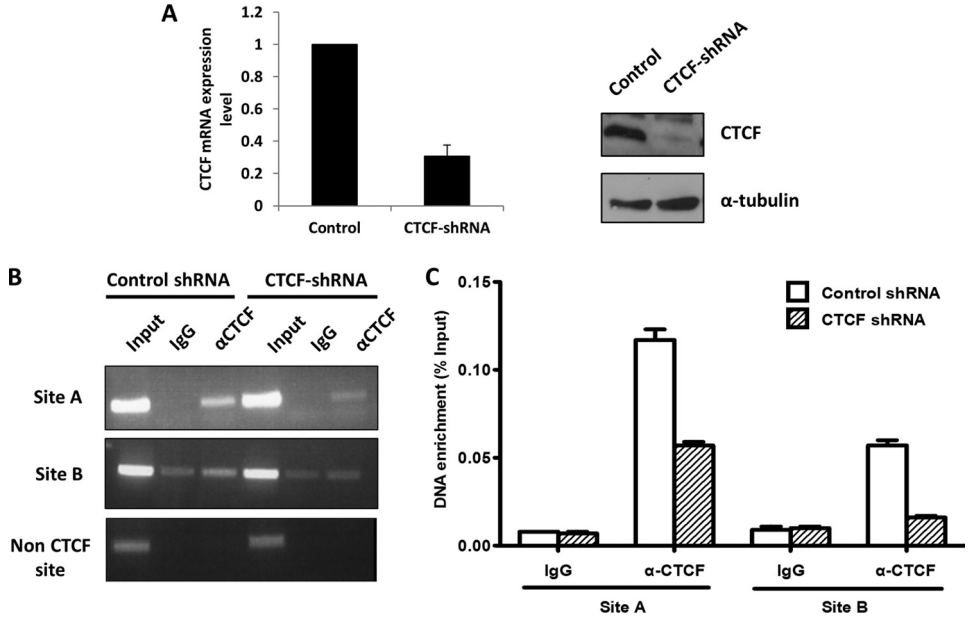

FIGURE 8. **Binding of CTCF at site A and site B in the two introns flanking ANG coding exon.** *A*, CTCF was knocked down by lentivirus-mediated shRNA in DU-145 cells, and a stable line was selected. *Left panel*, qRT-PCR analysis of mRNA level of CTCF in control and knockdown cell. *Right panels*, Western blot analysis of CTCF protein level. *B* and *C*, ChIP-PCR analyses of CTCF binding to site A and site B. Cells were treated with formaldehyde and immunoprecipitated with control or CTCF-specific antibodies. The precipitated DNA fragments was examined by regular PCR (*B*) or quantitative PCR (*C*) with primers specific to site A and site B.

down of CTCF decreased *ANG* and *RNASE4* transcript levels. Importantly, reporter gene expression promoted by *ANG* and *RNASE4* Pr-U was not affected by the cellular CTCF level (Fig. 10*D*), indicating that the effect of CTCF on *ANG* and *RNASE4* expression is gene-specific and is not a consequence of changes in overall transcription capacity.

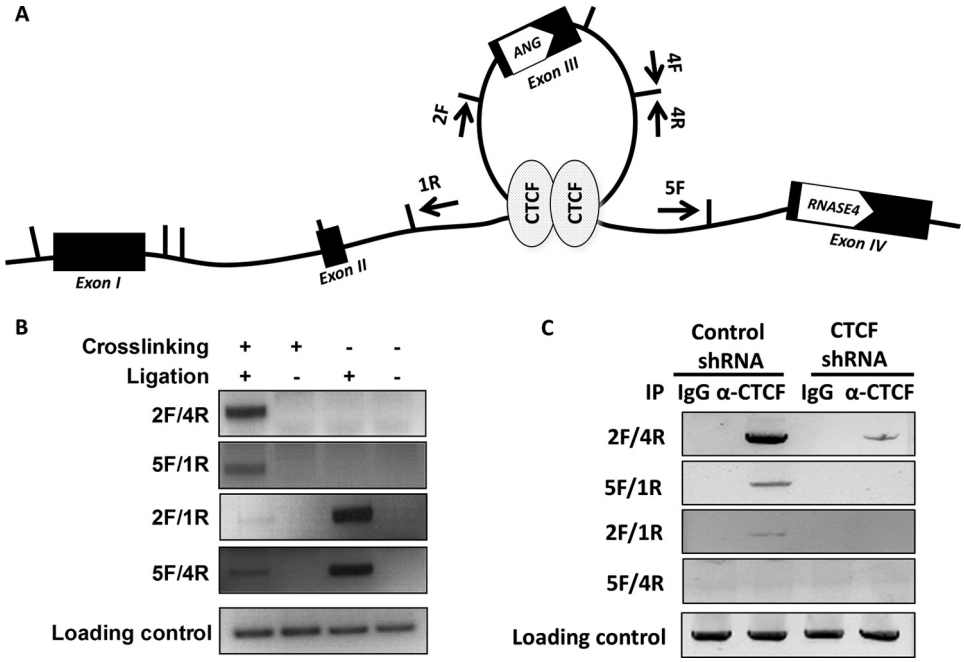

FIGURE 9. **Formation of a CTCF-dependent intragenic chromatin loop.** *A*, schematic view of a chromatin loop between the two introns flanking *ANG* coding exon. The *arrows* indicate the primers used in 3C experiment. *B*, chromatin loop formation shown by 3C assay. Transient chromatin interactions are stabilized by formaldehyde cross-linking followed by extraction and digestion with restriction enzyme StuI. DNA fragments were then ligated and amplified by PCR with the primer sets indicated in *A*. The loading control was derived from DNA sample before 3C with the primers amplifying the *ANG* coding region. *C*, ChIP-3C experiments. 3C and PCR amplifications were performed using control IgG and CTCF-specific IgG immunoprecipitated (*IP*) chromatin in both control and CTCF knockdown cells.

We have also examined the effect of CTCF overexpression on the mRNA levels of *ANG* and *RNASE4*. Two overexpression vectors were used: one with a V5-His tag at the C terminus and another with a FLAG-HA tag at the N terminus. The expression vectors were transfected in DU145 cells, and the transgene expression level was examined by immunoblot analyses with anti-His and anti-CTCF IgG (Fig. 11*A*). The mRNA levels of *ANG* and *RNASE4* were examined by qRT-PCR (Fig. 11*B*). The results indicated that CTCF overexpression enhanced *ANG* expression by ~70% but had no effect on *RNASE4* expression. Again, luciferase reporter gene expression promoted by Pr-U was not affected (Fig. 11*C*), confirming that the overall transcription capacity of the cells were not altered.

One possible mechanism by which CTCF overexpression differentially regulates the level of *ANG* and *RNASE4* mRNA could be through pausing of the Pol II elongation complex, which has been shown in both mammalian cells (47) and yeast (48). An intragenic chromatin loop may cause transcription pausing at the second CTCF site thereby increasing the possibility of transcription re-initiation and/or alternative splicing in favor of the inclusion of *ANG* coding exon in the transcript. If this hypothesis is true, there will be two transcripts: one contains only the *ANG* coding exon and the other contains both *ANG* and *RNASE4* exons. In this case, shRNA specific to *ANG* will knock down both transcripts, but that specific to *RNASE4* will only knock down the transcript-containing *RNASE4* coding exon. Fig. 11*D* shows that this was exactly the case. *ANG* shRNAs knocked down both *ANG* and *RNASE4*, whereas *RNASE4* shRNAs knock down only *RNASE4*.

DISCUSSION

We found that the $tRNA^{Tyr}$ and $tRNA^{Pro}$ genes located in the promoter region of the *ANG* and *RNAS4* gene locus influence the promoter activity in a reporter assay. Several genome-wide studies have shown that Pol II binds near many known Pol III genes and influences the expression of Pol III genes (49–51). It has been reported that tRNA elements can act as insulators (52) and that Pol III complexes can have an extratranscriptional function such as acting as a potential global chromatin bookmark to regulate gene expression patterns. We found that two Pol III genes ($tRNA^{Tyr}$ and $tRNA^{Pro}$) are located within the universal promoter of *ANG* and *RNASE4* gene locus and that both tRNA genes are actually occupied by Pol III complex including Pol III, TFIIIB, and TFIIIC. We further demonstrated that these fully occupied Pol III elements regulate Pol II gene transcription in a position- and orientation-dependent manner. When the Pol III elements are located downstream of the Pol II promoter, they inhibit the promoter activity. However, when they are located upstream of the Pol II promoter, they enhance the promoter activity. Both the enhancive and inhibitory activities require the Pol III elements to be in forward orientation. These results provide direct experimental evidence that Pol III-occupied genes could either suppress or enhance Pol II gene expression.

The reason for transcription-enhancing activity of Pol III elements located upstream of Pol II promoter could be a result of increased accessibility of Pol II components to the promoter. It is conceivable that juxtaposition of active Pol III transcription machinery with a Pol II promoter will create an open/active chromatin facilitating binding of Pol II components. However,

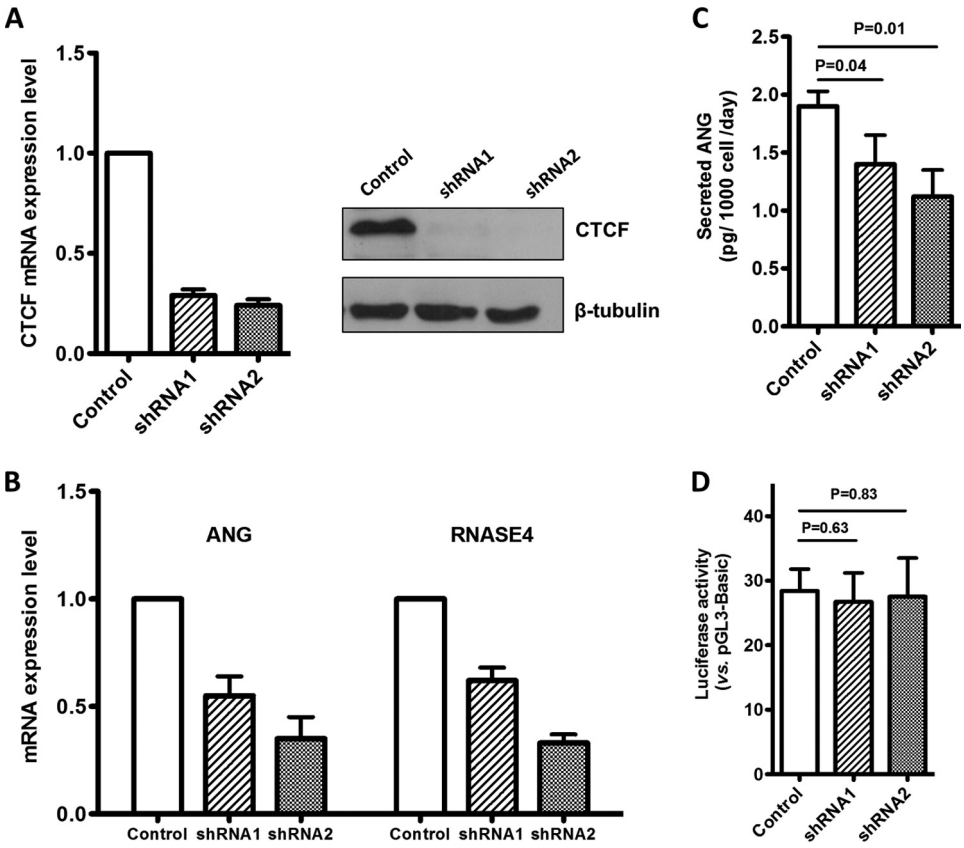

FIGURE 10. **Effect of CTCF knockdown on *ANG* and *RNASE4* transcription.** *A*, CTCF was knocked down by lentivirus-mediated shRNA in DU-145 cells, and stable knockdown cell lines were established after selection with 1 μg/ml puromycin for 7 days. *Left panel*, qRT-PCR analyses of CTCF mRNA level in control and shRNA transfected cell lines. CTCF mRNA level was normalized to that of β-actin. *Right panels*, Western blot analyses of CTCF protein level. *B*, qRT-PCR analyses of the mRNA levels of *ANG* and *RNASE4* in the three stable cells lines. *C*, ELISA analyses of secreted ANG protein from the stable control and CTCF knockdown cell lines. *D*, luciferase reporter activity of the full-length Pr-U in the above three stable cell lines. *Bar graphs* in all panels represent the means $\pm$ S.D. of three independent experiments.

when a Pol III complex is formed downstream of a Pol II promoter, it may serve as a physical barrier to prevent Pol II machinery from passing through the chromatin, thereby decreasing the overall transcription efficiency.

Another major finding of this study is that a CTCF-dependent intragenic chromatin loop formed between two introns and that this loop differentially regulates the transcription of *ANG* and *RNASE4*. The ENCODE project has identified tens of thousands of CTCF binding sites in a large number of human cell types, confirming on a genomic scale that CTCF is associated with both gene activation and repression (39). CTCF has been shown to interact with the initiation and elongation complexes of Pol II and to affect splicing (43). We identified two CTCF binding sites in the two introns flanking the ANG coding exon. Formation of such an inter-intron chromatin loop changes the chromatin structure of the *ANG* and *RNASE4* gene locus by looping out the *ANG* coding exon from a linear chromatin structure. We found that overexpression of CTCF enhanced the expression of only *ANG* but not *RNASE4*. These results revealed a new model of transcription regulation by CTCF. We speculated that overexpression of CTCF may result in formation of an excessive loop with a rigid chromatin that serves as a protein barrier causing transcription pausing at the second CTCF binding site. Paused transcription will alter the splicing of the transcript that preferentially favors the inclusion of the *ANG* coding exon because at this time the *RNASE4* exon has not yet been transcribed. It has been reported that a single CTCF binding site overlapping exon 5 of the *CD45* gene is associated with inclusion of exon 5 in *CD45* transcripts by affecting alternative splicing (47). Another possible mechanism for differential expression of *ANG* and *RNASE4* genes in CTCF overexpressing cells could be that transcription pausing at the end of the chromatin loop facilitates transcription re-initiation, which will result in exclusion of *RNASE4* coding exon from some of the transcripts. The observation that *ANG* shRNAs knock down expression of both *ANG* and *RNASE4*, whereas *RNASE4* shRNAs knock down only *RNASE4* supported this mechanism. Enhancement of *ANG* expression in *RNASE4* knockdown cells could be the result of a feedback effect that will selectively produce *ANG* mRNA based on the above proposed mode of action.

We have thus determined the transcription initiation site of the *ANG* and *RNASE4* genes, characterized the promoter sequences, and identified putative TFs and annotated potential biological pathways where ANG and RNASE4 could play a role. We have characterized the promoter activities and identified two potential mechanisms that regulate *ANG* and *RNASE4* expression. Although the Pol III elements control the general promoter activity that indiscriminately regulate *ANG* and *RNASE4* expression, a CTCF-dependent intragenic chromatin

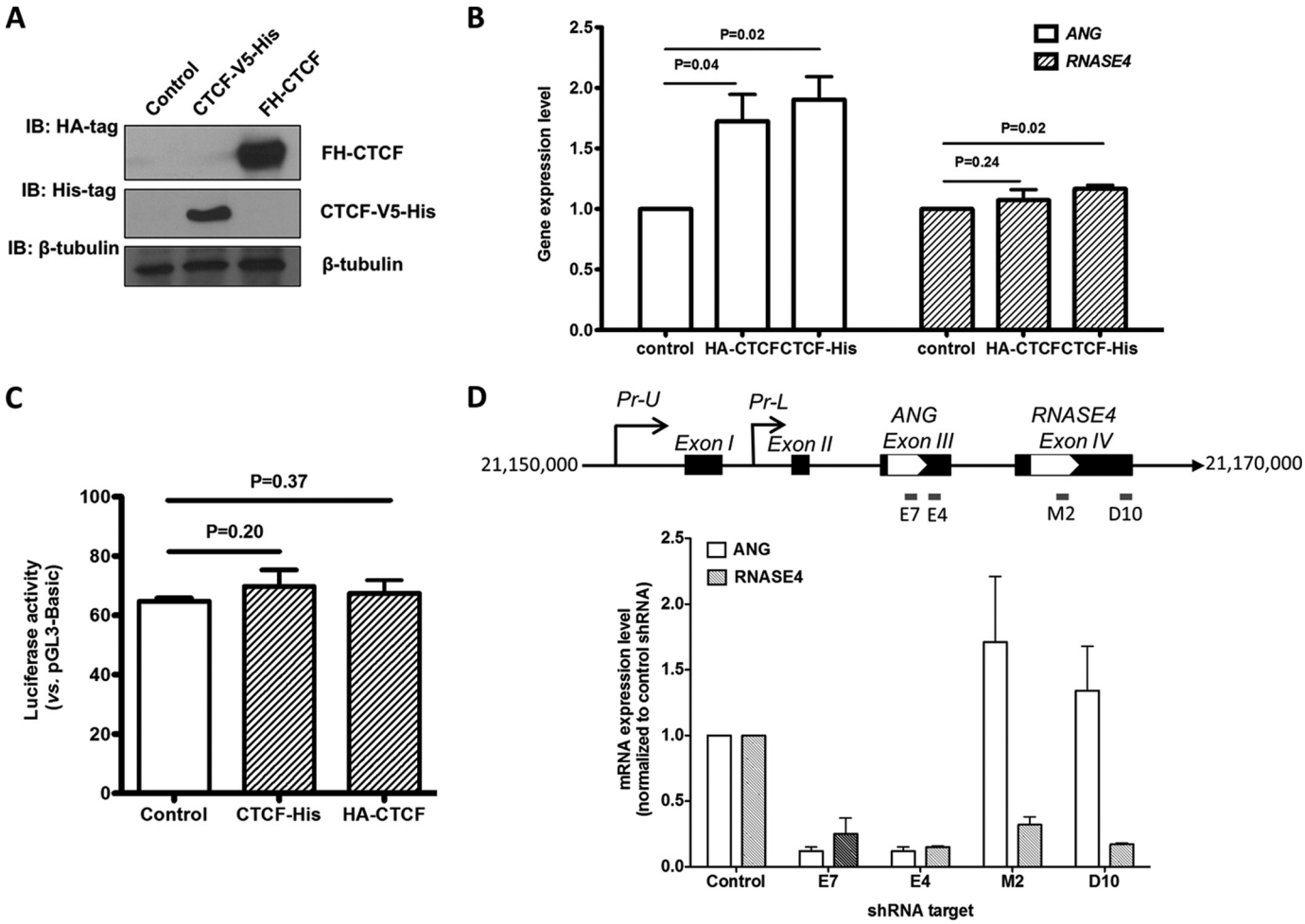

FIGURE 11. **Effect of CTCF overexpression on *ANG* and *RNASE4* expression.** *A*, overexpression of CTCF with V5-His tag or FLAG-HA tag in cells. The V5-His tag was fused to the C terminus of the CTCF, whereas the FLAG-HA was fused to the N terminus of the gene. The vectors were transfected to DU145 cells, and the cell lysates were analyzed for transgene expression by Western blot (*IB*) with antibodies specific to HA or His. *B*, qRT-PCR analyses of *ANG* and *RNASE4* mRNA level in CTCF-overexpressing cells. The mRNA level was first normalized to that of β-actin and then to control cell lines. The relative values to control cell line were shown. *C*, luciferase reporter activity of the full-length Pr-U construct in CTCF-overexpressing cell lines. The luciferase reporter construct was co-transfected with CTCF expression vector, and the luciferase activity was measured 48 h post transfection. *D*, effect of *ANG* and *RNASE4* shRNA on gene expression of the *ANG* and *RNASE4* locus. DU145 cells were infected by lentivirus particles encoding shRNA specific to *ANG* (E7 and E4) and *RNASE4* (M2 and D10) as indicated in the *top panel*. Stable cells lines were selected by 1 μg/ml puromycin for 7 days. mRNA levels of *ANG* and *RNASE4* were determined by qRT-PCR. mRNA levels were normalized to β-actin in the same sample. Data shown in the *bar graphs in all panels* are the means ± S.D. of three independent experiments.

loop differentially regulates *ANG* and *RNASE4* expression. These results indicate that even though *ANG* and *RNASE4* share the same promoter regions, they are not entirely co-expressed, suggesting that they have similar but distinct biological functions (23). Indeed, both ANG and RNASE4 have been shown to have angiogenic, neurogenic, and neuroprotective activities and play an important role in cancers and in neurodegenerative diseases. But there are important differences in their ribonucleolytic activities and substrate specificities. For example, RNASE4 has at least 30,000-fold higher ribonucleolytic activity than does ANG (22). Significantly, the K40A variant of RNASE4 in which the catalytically essential residue Lys-40 has been replaced by Ala actually has enhanced angiogenic activity (23). Moreover, RNASE4 has very strict substrate specificity. It strongly prefers a uridine at the 3′-side of the cleavage site (22), whereas ANG recognizes both uridine and pyrimidine residues. Differential regulation of *ANG* and *RNASE4* expression by the CTCF-dependent intragenic chromatin loop is thus in keeping with the subtle but distinct difference in the biological activities of the two proteins.

Acknowledgments—We thank Drs. Joaquin M. Espinosa of University of Colorado for providing human CTCF shRNA constructs, Recillas-Targa of USFC for providing pcDNA3.1 FL-CTCF-V5-His, and Dr. Felsenfeld G. of NIH for providing pOZ-FH-CTCF.

REFERENCES

1. Riordan, J. F. (2001) *Angiogenin. Methods Enzymol.* **341,** 263–273
2. Subramanian, V., and Feng, Y. (2007) A new role for angiogenin in neurite growth and pathfinding: implications for amyotrophic lateral sclerosis. *Hum. Mol. Genet* **16,** 1445–1453
3. Li, S., and Hu, G. F. (2010) Angiogenin-mediated rRNA transcription in cancer and neurodegeneration. *Int. J. Biochem. Mol. Biol.* **1,** 26–35
4. Tello-Montoliu, A., Patel, J. V., and Lip, G. Y. (2006) Angiogenin: a review of the pathophysiology and potential clinical applications. *J. Thromb. Haemost.* **4,** 1864–1874
5. Yoshioka, N., Wang, L., Kishimoto, K., Tsuji, T., and Hu, G. F. (2006) A

therapeutic target for prostate cancer based on angiogenin-stimulated angiogenesis and cancer cell proliferation. *Proc. Natl. Acad. Sci. U.S.A.* **103,** 14519–14524
6. Kishimoto, K., Liu, S., Tsuji, T., Olson, K. A., and Hu, G. F. (2005) Endogenous angiogenin in endothelial cells is a general requirement for cell proliferation and angiogenesis. *Oncogene* **24,** 445–456
7. Tsuji, T., Sun, Y., Kishimoto, K., Olson, K. A., Liu, S., Hirukawa, S., and Hu, G. F. (2005) Angiogenin is translocated to the nucleus of HeLa cells and is involved in ribosomal RNA transcription and cell proliferation. *Cancer Res.* **65,** 1352–1360
8. Li, S., Ibaragi, S., and Hu, G. F. (2011) Angiogenin as a molecular target for the treatment of prostate cancer. *Curr. Cancer Ther. Rev.* **7,** 83–90
9. McLaughlin, R. L., Phukan, J., McCormack, W., Lynch, D. S., Greenway, M., Cronin, S., Saunders, J., Slowik, A., Tomik, B., Andersen, P. M., Bradley, D. G., Jakeman, P., and Hardiman, O. (2010) Angiogenin levels and ANG genotypes: dysregulation in amyotrophic lateral sclerosis. *PLoS ONE* **5,** e15402
10. Steidinger, T. U., Standaert, D. G., and Yacoubian, T. A. (2011) A neuroprotective role for angiogenin in models of Parkinson's disease. *J. Neurochem.* **116,** 334–341
11. Kim, Y. N., and Kim, do H. (2012) Decreased serum angiogenin level in Alzheimer's disease. *Prog. Neuropsychopharmacol. Biol. Psychiatry* **38,** 116–120
12. Greenway, M. J., Andersen, P. M., Russ, C., Ennis, S., Cashman, S., Donaghy, C., Patterson, V., Swingler, R., Kieran, D., Prehn, J., Morrison, K. E., Green, A., Acharya, K. R., Brown, R. H., Jr., and Hardiman, O. (2006) ANG mutations segregate with familial and "sporadic" amyotrophic lateral sclerosis. *Nat. Genet.* **38,** 411–413
13. van Es, M. A., Schelhaas, H. J., van Vught, P. W., Ticozzi, N., Andersen, P. M., Groen, E. J., Schulte, C., Blauw, H. M., Koppers, M., Diekstra, F. P., Fumoto, K., LeClerc, A. L., Keagle, P., Bloem, B. R., Scheffer, H., van Nuenen, B. F., van Blitterswijk, M., van Rheenen, W., Wills, A. M., Lowe, P. P., Hu, G. F., Yu, W., Kishikawa, H., Wu, D., Folkerth, R. D., Mariani, C., Goldwurm, S., Pezzoli, G., Van Damme, P., Lemmens, R., Dahlberg, C., Birve, A., Fernández-Santiago, R., Waibel, S., Klein, C., Weber, M., van der Kooi, A. J., de Visser, M., Verbaan, D., van Hilten, J. J., Heutink, P., Hennekam, E. A., Cuppen, E., Berg, D., Brown, R. H., Jr., Silani, V., Gasser, T., Ludolph, A. C., Robberecht, W., Ophoff, R. A., Veldink, J. H., Pasterkamp, R. J., de Bakker, P. I., Landers, J. E., van de Warrenburg, B. P., and van den Berg, L. H. (2011) Angiogenin variants in Parkinson disease and amyotrophic lateral sclerosis. *Ann. Neurol.* **70,** 964–973
14. Wu, D., Yu, W., Kishikawa, H., Folkerth, R. D., Iafrate, A. J., Shen, Y., Xin, W., Sims, K., and Hu, G. F. (2007) Angiogenin loss-of-function mutations in amyotrophic lateral sclerosis. *Ann. Neurol.* **62,** 609–617
15. Emara, M. M., Ivanov, P., Hickman, T., Dawra, N., Tisdale, S., Kedersha, N., Hu, G. F., and Anderson, P. (2010) Angiogenin-induced tRNA-derived stress-induced RNAs promote stress-induced stress granule assembly. *J. Biol. Chem.* **285,** 10959–10968
16. Fu, H., Feng, J., Liu, Q., Sun, F., Tie, Y., Zhu, J., Xing, R., Sun, Z., and Zheng, X. (2009) Stress induces tRNA cleavage by angiogenin in mammalian cells. *FEBS Lett.* **583,** 437–442
17. Ivanov, P., Emara, M. M., Villen, J., Gygi, S. P., and Anderson, P. (2011) Angiogenin-induced tRNA fragments inhibit translation initiation. *Mol. Cell* **43,** 613–623
18. Yamasaki, S., Ivanov, P., Hu, G. F., and Anderson, P. (2009) Angiogenin cleaves tRNA and promotes stress-induced translational repression. *J. Cell Biol.* **185,** 35–42
19. Baird, S. D., Turcotte, M., Korneluk, R. G., and Holcik, M. (2006) Searching for IRES. *RNA* **12,** 1755–1785
20. Thompson, D. M., Lu, C., Green, P. J., and Parker, R. (2008) tRNA cleavage is a conserved response to oxidative stress in eukaryotes. *RNA* **14,** 2095–2103
21. Li, S., and Hu, G. F. (2012) Emerging role of angiogenin in stress response and cell survival under adverse conditions. *J. Cell. Physiol.* **227,** 2822–2826
22. Shapiro, R., Fett, J. W., Strydom, D. J., and Vallee, B. L. (1986) Isolation and characterization of a human colon carcinoma-secreted enzyme with pancreatic ribonuclease-like activity. *Biochemistry* **25,** 7255–7264
23. Li, S., Sheng, J., Hu, J. K., Yu, W., Kishikawa, H., Hu, M. G., Shima, K., Wu, D., Xu, Z., Xin, W., Sims, K. B., Landers, J. E., Brown, R. H., Jr., and Hu, G. F. (2013) Ribonuclease 4 protects neuron degeneration by promoting angiogenesis, neurogenesis, and neuronal survival under stress. *Angiogenesis* **16,** 387–404
24. Kieran, D., Sebastia, J., Greenway, M. J., King, M. A., Connaughton, D., Concannon, C. G., Fenner, B., Hardiman, O., and Prehn, J. H. (2008) Control of motoneuron survival by angiogenin. *J. Neurosci.* **28,** 14056–14061
25. Dyer, K. D., and Rosenberg, H. F. (2005) The mouse RNase 4 and RNase 5/ang 1 locus utilizes dual promoters for tissue-specific expression. *Nucleic Acids Res.* **33,** 1077–1086
26. Futami, J., Tsushima, Y., Murato, Y., Tada, H., Sasaki, J., Seno, M., and Yamada, H. (1997) Tissue-specific expression of pancreatic-type RNases and RNase inhibitor in humans. *DNA Cell Biol.* **16,** 413–419
27. Strydom, D. J. (1998) The angiogenins. *Cell. Mol. Life Sci.* **54,** 811–824
28. Gomes, N. P., and Espinosa, J. M. (2010) Gene-specific repression of the p53 target gene PUMA via intragenic CTCF-Cohesin binding. *Genes Dev.* **24,** 1022–1034
29. Yang, W., Ng, P., Zhao, M., Wong, T. K., Yiu, S. M., and Lau, Y. L. (2008) Promoter-sharing by different genes in human genome: CPNE1 and RBM12 gene pair as an example. *BMC Genomics* **9,** 456
30. Ernst, J., Kheradpour, P., Mikkelsen, T. S., Shoresh, N., Ward, L. D., Epstein, C. B., Zhang, X., Wang, L., Issner, R., Coyne, M., Ku, M., Durham, T., Kellis, M., and Bernstein, B. E. (2011) Mapping and analysis of chromatin state dynamics in nine human cell types. *Nature* **473,** 43–49
31. Sandelin, A., Carninci, P., Lenhard, B., Ponjavic, J., Hayashizaki, Y., and Hume, D. A. (2007) Mammalian RNA polymerase II core promoters: insights from genome-wide studies. *Nat. Rev. Genet* **8,** 424–436
32. Zambelli, F., Prazzoli, G. M., Pesole, G., and Pavesi, G. (2012) Cscan: finding common regulators of a set of genes by using a collection of genome-wide ChIP-seq datasets. *Nucleic Acids Res.* **40,** W510–W505
33. Ibaragi, S., Yoshioka, N., Kishikawa, H., Hu, J. K., Sadow, P. M., Li, M., and Hu, G.-F. (2009) Angiogenin-stimulated ribosomal RNA transcription is essential for initiation and survival of AKT-induced prostate intraepithelial neoplasia. *Mol. Cancer Res.* **7,** 415–424
34. Ibaragi, S., Yoshioka, N., Li, S., Hu, M. G., Hirukawa, S., Sadow, P. M., and Hu, G.-F. (2009) Neamine inhibits prostate cancer growth by suppressing angiogenin-mediated ribosomal RNA transcription. *Clin. Cancer Res.* **15,** 1981–1988
35. Katona, T. M., Neubauer, B. L., Iversen, P. W., Zhang, S., Baldridge, L. A., and Cheng, L. (2005) Elevated expression of angiogenin in prostate cancer and its precursors. *Clin. Cancer Res.* **11,** 8358–8363
36. Åberg, U. W., Saarinen, N., Abrahamsson, A., Nurmi, T., Engblom, S., and Dabrosin, C. (2011) Tamoxifen and flaxseed alter angiogenesis regulators in normal human breast tissue *in vivo*. *PLoS ONE* **6,** e25720
37. Nilsson, U. W., Abrahamsson, A., and Dabrosin, C. (2010) Angiogenin regulation by estradiol in breast tissue: tamoxifen inhibits angiogenin nuclear translocation and antiangiogenin therapy reduces breast cancer growth *in vivo*. *Clin. Cancer Res.* **16,** 3659–3669
38. Kanehisa, M., Araki, M., Goto, S., Hattori, M., Hirakawa, M., Itoh, M., Katayama, T., Kawashima, S., Okuda, S., Tokimatsu, T., and Yamanishi, Y. (2008) KEGG for linking genomes to life and the environment. *Nucleic Acids Res.* **36,** D480–D484
39. Lee, B. K., Bhinge, A. A., Battenhouse, A., McDaniell, R. M., Liu, Z., Song, L., Ni, Y., Birney, E., Lieb, J. D., Furey, T. S., Crawford, G. E., and Iyer, V. R. (2012) Cell-type specific and combinatorial usage of diverse transcription factors revealed by genome-wide binding studies in multiple human cells. *Genome Res.* **22,** 9–24
40. Phillips, J. E., and Corces, V. G. (2009) CTCF: master weaver of the genome. *Cell* **137,** 1194–1211
41. Ohlsson, R., Renkawitz, R., and Lobanenkov, V. (2001) CTCF is a uniquely versatile transcription regulator linked to epigenetics and disease. *Trends Genet.* **17,** 520–527
42. Chernukhin, I., Shamsuddin, S., Kang, S. Y., Bergström, R., Kwon, Y. W., Yu, W., Whitehead, J., Mukhopadhyay, R., Docquier, F., Farrar, D., Morrison, I., Vigneron, M., Wu, S. Y., Chiang, C. M., Loukinov, D., Lobanenkov, V., Ohlsson, R., and Klenova, E. (2007) CTCF interacts with and recruits the largest subunit of RNA polymerase II to CTCF target sites

genome-wide. *Mol. Cell Biol.* **27,** 1631–1648
43. Shukla, S., Kavak, E., Gregory, M., Imashimizu, M., Shutinoski, B., Kashlev, M., Oberdoerffer, P., Sandberg, R., and Oberdoerffer, S. (2011) CTCF-promoted RNA polymerase II pausing links DNA methylation to splicing. *Nature* **479,** 74–79
44. Luco, R. F., Allo, M., Schor, I. E., Kornblihtt, A. R., and Misteli, T. (2011) Epigenetics in alternative pre-mRNA splicing. *Cell* **144,** 16–26
45. Kim, T. H., Abdullaev, Z. K., Smith, A. D., Ching, K. A., Loukinov, D. I., Green, R. D., Zhang, M. Q., Lobanenkov, V. V., and Ren, B. (2007) Analysis of the vertebrate insulator protein CTCF-binding sites in the human genome. *Cell* **128,** 1231–1245
46. Dekker, J. (2006) The three Cs of chromosome conformation capture: controls, controls, controls. *Nat. Methods* **3,** 17–21
47. Fay, A., Misulovin, Z., Li, J., Schaaf, C. A., Gause, M., Gilmour, D. S., and Dorsett, D. (2011) Cohesin selectively binds and regulates genes with paused RNA polymerase. *Curr. Biol.* **21,** 1624–1634
48. O'Sullivan, J. M., Tan-Wong, S. M., Morillon, A., Lee, B., Coles, J., Mellor, J., and Proudfoot, N. J. (2004) Gene loops juxtapose promoters and terminators in yeast. *Nat. Genet.* **36,** 1014–1018
49. Barski, A., Chepelev, I., Liko, D., Cuddapah, S., Fleming, A. B., Birch, J., Cui, K., White, R. J., and Zhao, K. (2010) Pol II and its associated epigenetic marks are present at Pol III-transcribed noncoding RNA genes. *Nat. Struct. Mol. Biol.* **17,** 629–634
50. Oler, A. J., Alla, R. K., Roberts, D. N., Wong, A., Hollenhorst, P. C., Chandler, K. J., Cassiday, P. A., Nelson, C. A., Hagedorn, C. H., Graves, B. J., and Cairns, B. R. (2010) Human RNA polymerase III transcriptomes and relationships to Pol II promoter chromatin and enhancer-binding factors. *Nat. Struct. Mol. Biol.* **17,** 620–628
51. Raha, D., Wang, Z., Moqtaderi, Z., Wu, L., Zhong, G., Gerstein, M., Struhl, K., and Snyder, M. (2010) Close association of RNA polymerase II and many transcription factors with Pol III genes. *Proc. Natl. Acad. Sci. U.S.A.* **107,** 3639–3644
52. Van Bortle, K., and Corces, V. G. (2012) tDNA insulators and the emerging role of TFIIIC in genome organization. *Transcription* **3,** 277–284